Photothermal Infrared Spectroscopy of Airborne Samples with Mechanical String Resonators

ARTICLE *in* ANALYTICAL CHEMISTRY · OCTOBER 2013

Impact Factor: 5.64 · DOI: 10.1021/ac402585e · Source: PubMed

5 AUTHORS, INCLUDING:

Shoko Yamada
Technical University of Denmark
6 PUBLICATIONS **27** CITATIONS
SEE PROFILE

Silvan Schmid
Technical University of Denmark
54 PUBLICATIONS **635** CITATIONS
SEE PROFILE

Tom Larsen
Technical University of Denmark
9 PUBLICATIONS **65** CITATIONS
SEE PROFILE

Anja Boisen
Technical University of Denmark
276 PUBLICATIONS **4,851** CITATIONS
SEE PROFILE

analytical chemistry

Article

pubs.acs.org/ac

Photothermal Infrared Spectroscopy of Airborne Samples with Mechanical String Resonators

Shoko Yamada,*[,†] Silvan Schmid,[†] Tom Larsen,[†,§] Ole Hansen,[†,‡] and Anja Boisen[†]

[†]Department of Micro- and Nanotechnology, Technical University of Denmark, 2800 Kgs. Lyngby, Denmark

[‡]Center for Individual Nanoparticle Functionality, Technical University of Denmark, 2800 Kgs. Lyngby, Denmark

Supporting Information

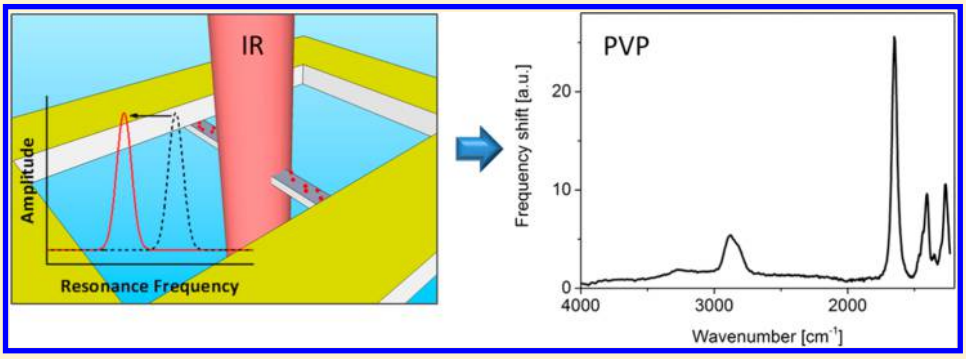

ABSTRACT: Micromechanical photothermal infrared spectroscopy is a promising technique, where absorption-related heating is detected by frequency detuning of microstring resonators. We present photothermal infrared spectroscopy with mechanical string resonators providing rapid identification of femtogram-scale airborne samples. Airborne sample material is directly collected on the microstring with an efficient nondiffusion limited sampling method based on inertial impaction. Resonance frequency shifts, proportional to the absorbed heat in the microstring, are recorded as monochromatic IR light is scanned over the mid-infrared range. As a proof-of-concept, we sample and analyze polyvinylpyrrolidone (PVP) and the IR spectrum measured by photothermal spectroscopy matches the reference IR spectrum measured by an FTIR spectrometer. We further identify the organic surface coating of airborne TiO_2 nanoparticles with a total mass of 4 pg. With an estimated detection limit of 44 fg, the presented sensor demonstrates a new paradigm in ultrasensitive vibrational spectroscopy for identification of airborne species.

Micro and nanoelectromechanical resonators have offered a range of highly sensitive mass sensors,[1−6] but obtaining good specificity is generally challenging. Such gravimetric sensors lack intrinsic selectivity and typically rely on selective interfaces for chemical specificity.[7,8] Spectroscopy techniques offer a simple and sensitive way to chemically analyze a sample and are therefore widely used in science and industry. The chemical information is obtained by measuring a unique interaction of the sample matter with a defined emitted energy. Detection of the unique spectrum of an analyte by infrared (IR) absorption spectroscopy can be a solution to the specificity problem when performing chemical analysis of increasingly smaller sample volumes.

In absorption spectroscopy, the energy absorbed by the sample is usually directly determined by measuring the fraction of light being transmitted through the sample. IR spectroscopy in the mid-infrared region provides information on molecular vibrations that result in a sample specific absorption spectrum, the so-called fingerprint. A minimum sample mass of 0.25 mg and additional 100 mg potassium bromide (KBr) are typically needed for preparing a micropellet for transmission measurements with Fourier transform IR spectroscopy (FTIR).[9] It has been shown that femtogram-level paraffin can be sampled on an AFM microprobe and subsequently analyzed with an FTIR microspectrometer.[10] Another way is to determine the absorbed energy indirectly by measuring the absorption-related heating of the sample. This so-called photothermal spectroscopy is sensitive enough to study optically thin samples. It has been shown that photothermal absorption spectroscopy can be implemented as a mechanical sensor. By measuring the bending of a bilayer cantilever (metal layer on silicon or silicon nitride cantilever) due to photothermal heating, the sensitivity was increased by 2 orders of magnitude compared to standard photothermal deflection spectroscopy.[11,12] The cantilever-based photothermal spectroscopy has been applied for detecting chemicals,[13−15] biomolecules,[16] trace explosives,[17,18] and chemical warfare agents[19,20] and for investigating polymer thin films.[21,22] However, the cantilever deflection is directly subjected to thermomechanical noise and external vibrations.

In this paper, we present a novel photothermal IR spectroscopy technique, where mechanical string resonators are used as thermal sensors by monitoring the temperature-

Received: August 14, 2013
Accepted: October 1, 2013
Published: October 1, 2013

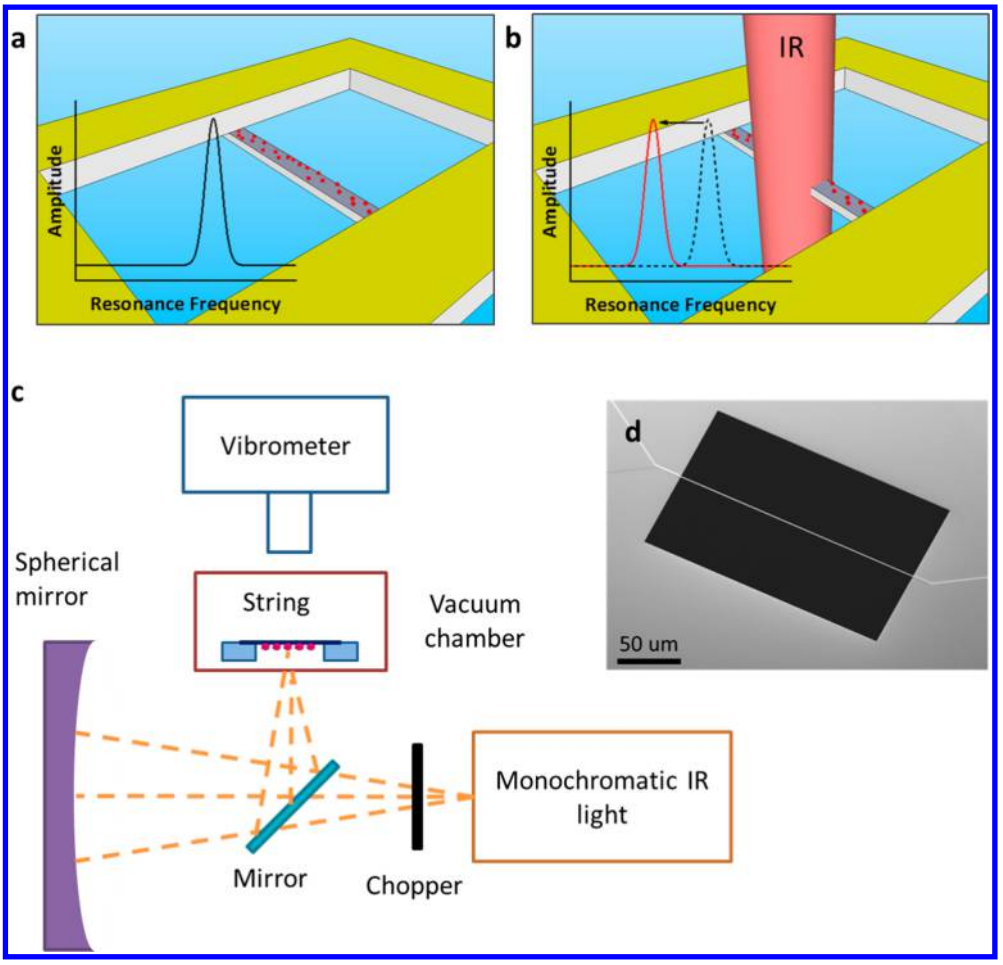

Figure 1. Shematic drawings explaining photothermal IR spectroscopy with mechanical string resonator with in situ nondiffusion limited sampling. (a) Airborne species are deposited on the string by the aerosol flowing through the chip thereby passing the string resonator. The airborne species are then efficiently collected on the string mainly by inertial impaction. (b) Collected species are excited into vibration modes by absorption of IR photons causing a photothermal heating. The thermal energy is then transferred to the string resulting in a frequency detuning. (c) Experimental setup used for the photothermal measurements. The string is placed at the focal point of the spherical mirror. A chopper is used to obtain a frequency shift signal caused by the absorbed IR light. (d) Scanning electron microscope image of a typical string resonator used in this work. It is a 213 μm long, 981 nm wide, and 185 nm thick silicon nitride string.

induced frequency detuning.[23−26] Strings allow for a simple fabrication (a single material clamped at both ends), a robust detection scheme (measuring frequency detuning), and a minimum heat dissipation (no metals required and large aspect ratio). Finally, strings facilitate simple nondiffusion limited analyte sampling.[3]

The responsivity of chemical or biochemical sensors is strongly dependent on the sample collection efficiency.[27] The probability of nanoscale sample entities to stick to a micro- or nanoscale sensor surface by diffusion is very low, which results in long sampling times.[28] For many sensor applications, the available sample concentration is however below the detection limit. This problem is commonly overcome by performing a preconcentration of the analyte. Sample preparation and preconcentration are not only time-consuming but also contribute about 30% to the error in the total analysis of a sample.[29] In our photothermal sensor, we apply an efficient nondiffusion limited sampling method in which airborne species are directly collected on the mechanical string resonator with an up to 100% collection efficiency of the species that are flowing in the projection of the string resonator.[3,30]

The string spectrometer thus fulfills two core roles as: (i) sampling/preconcentrating element and (ii) thermally isolated ultrasensitive temperature-sensing element. Once the airborne analyte is collected on the string, it is exposed to IR radiation from a scanning monochromator. Figure 1a,b schematically depict the principle of photothermal IR spectroscopy, and the experimental system is shown in Figure 1c. A string vibrates at its resonance frequency, as shown in Figure 1a, and it vibrates at a lower resonance frequency when the string is heated by the absorbed heat of the sample, as shown in Figure 1b. The resonance frequency shift, detected by optical readout, is proportional to the heat flux into the string. Therefore, IR spectra measured by photothermal spectroscopy recorded while the monochromator is scanning are similar to IR spectra measured by an FTIR spectrometer and contain a superposition of characteristic vibrational signatures of the chemical entities in the sample.

The mechanical string resonators were fabricated from low-stress silicon nitride by standard cleanroom processing, as described by Schmid et al.[31] Silicon nitride is not entirely transparent for IR light. Thus, in a first experiment the IR spectrum of a bare silicon nitride resonator measured by

photothermal spectroscopy is recorded. The experimental details are described in the Supporting Information.

RESULTS AND DISCUSSION

Figure 2a shows an IR spectrum of a bare silicon nitride string measured by photothermal spectroscopy, showing a strong and

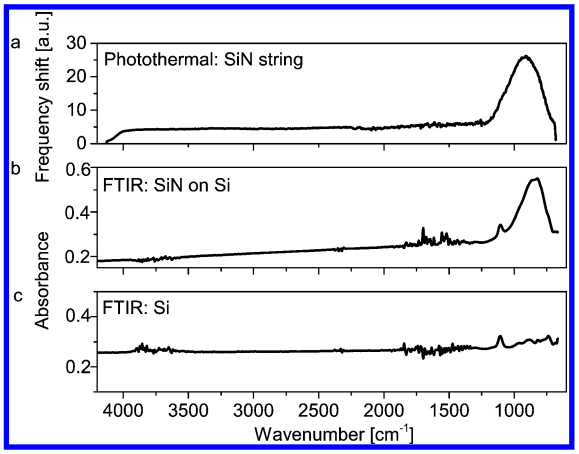

Figure 2. Analysis of bare silicon nitride string resonators. (a) IR spectrum of a 509 μm long, 5.4 μm wide, and 185 nm thick silicon nitride string measured by photothermal spectroscopy. (b) IR spectrum of a 185 nm thick silicon nitride film deposited on a 350 μm thick double side polished silicon wafer measured by an FTIR spectrometer. (c) IR spectrum of a 350 μm thick double side polished silicon wafer measured by an FTIR spectrometer.

broad absorption peak at 904 cm^{-1}. This peak position has been verified by means of conventional FTIR spectroscopy. Figure 2b,c show the IR spectra of a silicon wafer and a silicon wafer with a 185 nm thick silicon nitride layer measured by an FTIR spectrometer. From these two IR spectra, it can be deduced that the silicon nitride layer has an absorption peak at 895 cm^{-1}. Silicon nitride is known to have an absorption peak at 830−1250 cm^{-1}, depending on the thickness of the silicon nitride. The absorption peak is shifted to longer wavelengths when the thickness of the silicon nitride is reduced.[32] This absorption is caused by stretching of Si−N bonds, and the peak position is in good agreement with the position determined by photothermal IR spectroscopy. Figure 2b,c also show an absorption peak at 1106 cm^{-1}, deriving from silicon. The absorption peaks at 1400−1800 and 3600−4000 cm^{-1} derive from water vapor, and the absorption peak at 2350 cm^{-1} derives from carbon dioxide since these samples were measured in air.

Biodegradable polymers are becoming increasingly used,[33,34] and there is a large demand for polymer characterization and identification. PVP was atomized, and the resulting aerosol was sampled on a string resonator. In Figure 3a,b, IR spectra of PVP deposited on two different strings measured by photothermal spectroscopy show the repeatability of the measurement. It can be seen that the two IR spectra of PVP from two different strings measured by photothermal spectroscopy are highly reproducible. All the four major absorption peaks in the IR spectra measured by photothermal spectroscopy at 1267, 1407, 1651, and 2878 cm^{-1} are in excellent agreement with the reference IR spectrum of PVP measured by an FTIR spectrometer in air, showing major absorption peaks at 1285, 1422, 1651, and 2951 cm^{-1} (Figure 3c). The distinct peak at 1651 cm^{-1} is coming from the carbonyl double bond in PVP.

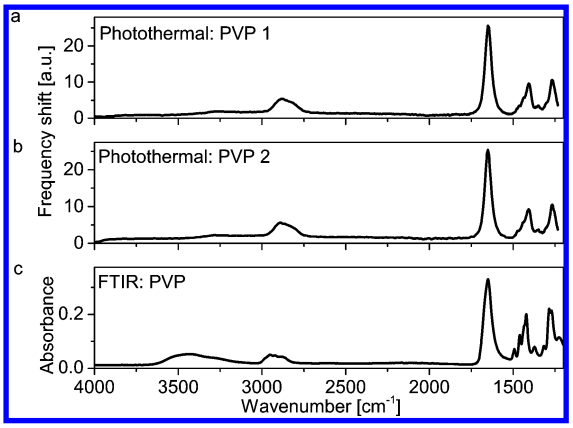

Figure 3. PVP analysis. (a) IR spectrum of PVP (with a total mass of 583 pg) on a silicon nitride string (506 μm long, 3 μm wide, and 157 nm thick) measured by photothermal spectroscopy. (b) IR spectrum of PVP on a different silicon nitride string of equal dimensions measured by photothermal spectroscopy. (c) IR spectrum of PVP measured by an FTIR spectrometer.

The extra absorption peak at 3428 cm^{-1} of the FTIR measurement comes from water vapor.

Analysis of airborne nanoparticles is a common scenario in the field of environmental and workplace safety.[35] Chemical identification of airborne nanoparticles typically requires an electron microscope featuring an energy-dispersive X-ray spectrometer and is therefore time-consuming and expensive.[35,36] The combination of efficient in situ sampling and photothermal IR spectroscopy is very attractive for chemical analysis of airborne engineered nanoparticles. The often-used organic surface coating of engineered nanoparticles has shown to play a major role in the toxicity of nanoparticles.[37] It is therefore highly desired to be able to detect and distinguish surface coatings of nanoparticles. Figure 4 shows the differential IR spectrum of TiO_2 nanoparticles with and without coating measured by photothermal spectroscopy. It can clearly be seen that the spectrum of TiO_2 with coating has two extra peaks at 1597 and 3389 cm^{-1}. The coating on the TiO_2 nanoparticles contains glycerol, tetramethyl silicate, hexadecanoic acid methyl ester, and octadecanoic acid methyl ester as major substances.

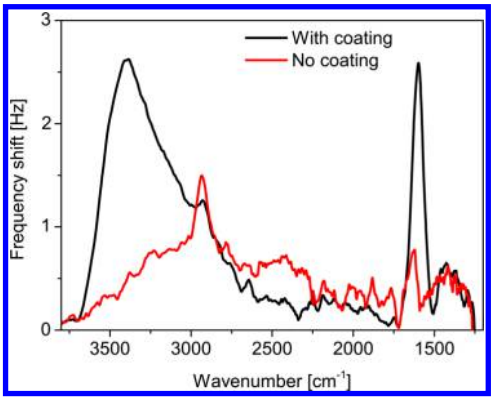

Figure 4. Identification of organic nanoparticle coating. Differential IR spectra of 20 nm TiO_2 nanoparticles (with a total mass of 200 pg) with and without organic coating measured with a 512 μm long, 3 μm wide, and 185 nm thick silicon nitride string measured by photothermal spectroscopy. The coating with a total mass of 4 pg is mainly composed of glycerol, tetramethyl silicate, hexadecanoic acid methyl ester, and octadecanoic acid methyl ester.

dx.doi.org/10.1021/ac402585e | Anal. Chem. 2013, 85, 10531−10535

The broad peak at 3389 cm^{-1} is typical from the stretching vibrations of O−H bonds that are present in the glycerol of the particle coating. The sharp peak at 1597 cm^{-1} could be coming from the stretching of the double bonds in the two different ester compounds. According to the specifications, the weight of the coating was 2% of the mass of the nanoparticles. This results in a total coating mass of 4 pg for a total TiO_2 nanoparticle mass of 200 pg.

For the presented measurements, an IR monochromator with a thermal light source has been used. The power of radiated light absorbed by the micromechanical string resonator is estimated from the measurement of the bare silicon nitride string. The absolute frequency shift of silicon nitride of −13.1 Hz at 904 cm^{-1} (Figure 2a) corresponds to a relative frequency shift of 52.5 ppm. The relative resonance frequency change of a mechanical string resonator (with length L and cross section area A) as a function of the absorbed power P in the string center is given by (see Supporting Information)

$$\frac{\Delta f}{f} = -\frac{\alpha E}{\sigma_0 k}\frac{L}{16A}P \quad (1)$$

with Young's modulus E, thermal expansion coefficient α, tensile prestress σ_0, and thermal conductivity κ, of the string material. From eq 1, it is calculated that the measured frequency shift corresponds to approximately 2.7 nW of absorbed heat in the string. The absorbance of silicon nitride can be extracted from the FTIR measurements by subtracting the absorbance of bare silicon (Figure 2c) from the absorbance of silicon nitride on a silicon wafer (Figure 2b). A differential absorbance of 0.196 can be calculated at 904 cm^{-1}, which results in an IR power radiated on the string of approximately 14 nW. The calculations were done assuming the following parameters: tensile stress 200 MPa, mass density 3100 kg/m^3, thermal coefficient of expansion 1.23 ppm/K,[23] Young's modulus 250 GPa, and thermal conductivity 2.5 W/(m K).[38]

A noise value is required to estimate the detection limit of the sensor. The noise comes mainly from temperature drift in the chamber and power fluctuation in the readout laser. We have calculated the Allan deviations of frequency versus time measurements for three scenarios using an uncoated string: (i) without IR light, (ii) with IR light at 1176 cm^{-1} where there is low absorption in silicon nitride, and (iii) with IR light at 909 cm^{-1} where there is high absorption in silicon nitride. Allan deviations of $\sigma(1s) \approx 1.2 \times 10^{-7}$, $\sigma(1s) \approx 1.1 \times 10^{-7}$, and $\sigma(1s) \approx 1.3 \times 10^{-7}$ were obtained from the respective measurements. It can be seen that IR radiation does not change the Allan deviation. From the Allan deviation of $\sigma(1s) \approx 1.1 \times 10^{-7}$ and the relative frequency change of 20 786 W^{-1}, the detection limit is calculated to be approximately 16 pW for a signal-to-noise ratio of 3. This is similar to that of more complex bimaterial cantilevers with a typical detection limit of 12 pW for the same signal-to-noise ratio.[39,40]

The minimum detectable sample mass can be estimated from the maximum induced frequency shift of ∼2.6 Hz (see Figure 4) for a mass of 4 pg. This relates to a relative frequency change of roughly 2.5×10^6 g^{-1}, which results in a minimum detectable mass of 44 fg with an Allan deviation of 1.1×10^{-7}. Considering the linear relationship of photothermally induced frequency detuning and radiated light power, the estimated femtogram-scale mass resolution for nW-scale radiation power is well in agreement with the attogram-scale resolution obtained with similar mechanical resonators irradiated with a visible μW laser.[24] The sensitivity of the presented photothermal IR spectroscopy can be improved by several orders of magnitude by replacing the weak thermal IR source and monochromator with a more powerful light source. Modern tunable quantum cascade lasers provide IR powers of up to several 100 mW, which could enable measurements at atmospheric pressure in the future. Additionally, the sensitivity can be enhanced by optimizing the string design according to the analytical model (1) (e.g., longer strings with smaller cross-section area). The combination of an optimized string design and stronger radiation power gives prospect to photothermal IR spectroscopy in the zeptogram range.

CONCLUSIONS

In conclusion, we have performed the first photothermal IR spectroscopy with mechanical string resonators for chemical identification of airborne species. We have demonstrated that the obtained IR spectra measured by photothermal spectroscopy match the state-of-the-art IR spectra measured by an FTIR spectrometer. Airborne species can directly be collected on the string resonator by means of in situ nondiffusion limited sampling. Therewith, we identified the organic coating of airborne nanoparticles, with a mass of 4 pg. It is estimated that the current femtogram-scale mass resolution can be enhanced to the zeptogram-scale by means of an optimal string design and increased IR light power.

ASSOCIATED CONTENT

Supporting Information

Additional information as noted in the text. This material is available free of charge via the Internet at http://pubs.acs.org

AUTHOR INFORMATION

Corresponding Author

*E-mail: syam@nanotech.dtu.dk.

Present Address

[§]Microsystems Laboratory, Stanford University, 496 Lomita Mall, Durand 102, Stanford, CA 94305.

Author Contributions

S.Y. designed and performed the experiments. T.L. assisted in the design and conduction of the experiments. S.S. and A.B. supervised the work. O.H. developed the analytical model. All authors contributed to the writing of the article.

Notes

The authors declare no competing financial interest.

ACKNOWLEDGMENTS

We would like to thank Seonghwan Kim and Thomas Thundat for the help with photothermal measurement setup. The research leading to these results has received funding from the European Community's Seventh Framework Programme (FP7/2007-2013) under Grant Agreement No. 211464-2. This work was partly supported by the Danish National Research Foundation's Center for Individual Nanoparticle Functionality (DNRF54).

REFERENCES

(1) Hanay, M.; Kelber, S.; Naik, A.; Chi, D.; Hentz, S.; Bullard, E.; Colinet, E.; Duraffourg, L.; Roukes, M. *Nat. Nanotechnol.* **2012**, *7* (9), 602−608.

(2) Yang, Y.; Callegari, C.; Feng, X.; Ekinci, K.; Roukes, M. *Nano Lett.* **2006**, *6* (4), 583−586.

(3) Schmid, S.; Kurek, M.; Adolphsen, J. Q.; Boisen, A. *Sci. Rep.* **2013**, *3*, 1288−1288/5.
(4) Chaste, J.; Eichler, A.; Moser, J.; Ceballos, G.; Rurali, R.; Bachtold, A. *Nat. Nanotechnol.* **2012**, *7*, 301−304.
(5) Jensen, K.; Kim, K.; Zettl, A. *Nat. Nanotechnol.* **2008**, *3* (9), 533−537.
(6) Burg, T. P.; Godin, M.; Knudsen, S. M.; Shen, W.; Carlson, G.; Foster, J. S.; Babcock, K.; Manalis, S. R. *Nature* **2007**, *446* (7139), 1066−1069.
(7) Grate, J. W. *Chem. Rev.* **2000**, *100* (7), 2627−2648.
(8) Grate, J. W.; Martin, S. J.; White, R. M. *Anal. Chem.* **1993**, *65* (21), 940A−948A.
(9) Solomon, P. R.; Carangelo, R. M. *Fuel* **1982**, *61* (7), 663−669.
(10) Park, K.; Lee, J.; Bhargava, R.; King, W. P. *Anal. Chem.* **2008**, *80* (9), 3221−3228.
(11) Barnes, J. R.; Stephenson, R. J.; Welland, M. E.; Gerber, C.; Gimzewski, J. K. *Nature* **1994**, *372* (6501), 79−81.
(12) Barnes, J.; Stephenson, R.; Woodburn, C.; Oshea, S.; Welland, M.; Rayment, T.; Gimzewski, J.; Gerber, C. *Rev. Sci. Instrum.* **1994**, *65* (12), 3793−3798.
(13) Li, G.; Burggraf, L. W.; Baker, W. P. *Appl. Phys. Lett.* **2000**, *76* (9), 1122−1124.
(14) Datskos, P. G.; Rajic, S.; Sepaniak, M. J.; Lavrik, N.; Tipple, C. A.; Senesac, L. R.; Datskou, I. *J. Vac. Sci. Technol., B: Microelectron. Process. Phenom.* **2001**, *19* (4), 1173−1179.
(15) Datskos, P.; Sepaniak, M.; Tipple, C.; Lavrik, N. *Sens. Actuators, B* **2001**, *76* (1), 393−402.
(16) Arakawa, E. T.; Lavrik, N. V.; Rajic, S.; Datskos, P. G. *Ultramicroscopy* **2003**, *97* (1), 459−466.
(17) Krause, A. R.; Van Neste, C.; Senesac, L.; Thundat, T.; Finot, E. *J. Appl. Phys.* **2008**, *103* (9), 094906−094906/6.
(18) Senesac, L.; Thundat, T. G. *Mater. Today* **2008**, *11* (3), 28−36.
(19) Arakawa, E. T.; Lavrik, N. V.; Datskos, P. G. *Appl. Opt.* **2003**, *42* (10), 1757−1762.
(20) Wig, A.; Arakawa, E. T.; Passian, A.; Ferrell, T. L.; Thundat, T. *Sens. Actuators, B* **2006**, *114* (1), 206−211.
(21) Yun, M.; Kim, S.; Lee, D.; Jung, N.; Chae, I.; Jeon, S.; Thundat, T. *Appl. Phys. Lett.* **2012**, *100* (20), 204103−204103/4.
(22) Kim, S.; Lee, D.; Yun, M.; Jung, N.; Jeon, S.; Thundat, T. *Appl. Phys. Lett.* **2013**, *102* (2), 024103−024103/4.
(23) Larsen, T.; Schmid, S.; Gronberg, L.; Niskanen, A.; Hassel, J.; Dohn, S.; Boisen, A. *Appl. Phys. Lett.* **2011**, *98* (12), 121901−121901/3.
(24) Larsen, T.; Schmid, S.; Villanueva, L. G.; Boisen, A. *ACS Nano* **2013**, *7* (7), 6188−6193.
(25) Larsen, T.; Schmid, S.; Boisen, A. *AIP Conference Proceedings* **2013**, *931*, 1552 DOI: 10.1063/1.4819669.
(26) Zhang, X.; Myers, E. B.; Sader, J. E.; Roukes, M. L. *Nano Lett.* **2013**, *13* (4), 1528−1534.
(27) Lin, E.-C.; Fang, J.; Park, S.-C.; Johnson, F. W.; Jacobs, H. O. *Nat. Commun.* **2013**, *4*, 1636−1636/8.
(28) Squires, T. M.; Messinger, R. J.; Manalis, S. R. *Nat. Biotechnol.* **2008**, *26* (4), 417−426.
(29) Papadoyannis, I. N.; Samanidou, V. F. In *Encyclopedia of Chromatography*; Cazes, J., , Ed.; Taylor & Francis, LLC: Boca Raton, FL, **2004**; pp 250−266.
(30) Schmid, S.; Kurek, M.; Boisen, A. In *Proceedings of SPIE*; SPIE—The International Society for Optical Engineering, 2013; *8725*.
(31) Schmid, S.; Jensen, K. D.; Nielsen, K. H.; Boisen, A. *Phys. Rev. B* **2011**, *84* (16), 165307−165307/5.
(32) Wicaksono, D. H. B.; Pandraud, G.; French, P. J.; Jutzi, F. In *Proceedings of IEEE Sensors*; IEEE, 2008; pp 498−501.
(33) Guan, J.; Fujimoto, K. L.; Sacks, M. S.; Wagner, W. R. *Biomaterials* **2005**, *26* (18), 3961−3971.
(34) Amass, W.; Amass, A.; Tighe, B. *Polym. Int.* **1998**, *47* (2), 89−144.
(35) Kuhlbusch, T.; Asbach, C.; Fissan, H.; Göhler, D.; Stintz, M. *Part. Fibre Toxicol.* **2011**, *8* (22), 1−18.
(36) Marquis, B. J.; Love, S. A.; Braun, K. L.; Haynes, C. L. *Analyst* **2009**, *134* (3), 425−439.
(37) Saber, A. T.; Jensen, K. A.; Jacobsen, N. R.; Birkedal, R.; Mikkelsen, L.; Møller, P.; Loft, S.; Wallin, H.; Vogel, U. *Nanotoxicology* **2012**, *6* (5), 453−471.
(38) Alam, M.; Manoharan, M.; Haque, M.; Muratore, C.; Voevodin, A. *J. Micromech. Microeng.* **2012**, *22* (4), 045001−045001/8.
(39) Sadat, S.; Chua, Y. J.; Lee, W.; Ganjeh, Y.; Kurabayashi, K.; Meyhofer, E.; Reddy, P. *Appl. Phys. Lett.* **2011**, *99* (4), 043106−043106/3.
(40) Varesi, J.; Lai, J.; Perazzo, T.; Shi, Z.; Majumdar, A. *Appl. Phys. Lett.* **1997**, *71* (3), 306−308.